Burst-duration mechanism of in-phase bursting in inhibitory networks

Article *in* Regular and Chaotic Dynamics · June 2010

DOI: 10.1134/S1560354710020048

3 authors, including:

Igor Belykh
Georgia State University
93 PUBLICATIONS **3,362** CITATIONS

SEE PROFILE

Andrey Shilnikov
Georgia State University
213 PUBLICATIONS **4,038** CITATIONS

SEE PROFILE

ISSN 1560-3547, Regular and Chaotic Dynamics, 2010, Vol. 15, No. 2–3, pp. 148–160. © Pleiades Publishing, Ltd., 2010.

ARTICLES

Burst-Duration Mechanism of In-phase Bursting in Inhibitory Networks

I. Belykh[1, 2*], S. Jalil[1, 2], and A. Shilnikov[2, 1***]**

[1] *Department of Mathematics and Statistics, Georgia State University, 30 Pryor Street, Atlanta, GA 30303, USA*

[2] *Neuroscience Institute, Georgia State University, 30 Pryor Street, Atlanta, GA 30303, USA*

Received December 19, 2009; accepted December 26, 2009

Abstract—We study the emergence of in-phase and anti-phase synchronized rhythms in bursting networks of Hodgkin–Huxley–type neurons connected by inhibitory synapses. We show that when the state of the individual neuron composing the network is close to the transition from bursting into tonic spiking, the appearance of the network's synchronous rhythms becomes sensitive to small changes in parameters and synaptic coupling strengths. This bursting-spiking transition is associated with codimension-one bifurcations of a saddle-node limit cycle with homoclinic orbits, first described and studied by Leonid Pavlovich Shilnikov. By this paper, we pay tribute to his pioneering results and emphasize their importance for understanding the cooperative behavior of bursting neurons. We describe the burst-duration mechanism of in-phase synchronized bursting in a network with strong repulsive connections, induced by weak inhibition. Through the stability analysis, we also reveal the dual property of fast reciprocal inhibition to establish in- and anti-phase synchronized bursting.

MSC2000 numbers: ??

DOI: 10.1134/S1560354710020048

Key words: ??

Dedicated to Leonid P. Shilnikov on the occasion of his 75th birthday

1. INTRODUCTION

The theory of dynamical systems has proven useful in gaining new insights into how neural systems operate, and has made predictions that have aided in the design of new experiments [1–35]. A central problem in these studies is to understand how single neuron dynamics contributes to network oscillations and spatio-temporal pattern formation. Neurons can generate a complex oscillatory rhythm known as bursting, which occurs when neuron activity alternates, on a slow time scale, between a quiescent state and fast repetitive spiking. The intrinsic mechanisms that generate and control bursting oscillations have recently received a great deal of attention [1–15]. Interacting bursting neurons may exhibit different forms of synchrony; including synchronization of individual spikes, burst synchronization when only the envelopes of the spikes synchronize, complete synchrony and anti-phase bursting. Inhibitory and excitatory synapses play different roles in promoting synchronization or anti-synchronization of bursting neurons [16–35]. It has been shown that the synchronizing roles of inhibition and excitation depend on the rates of onset and decay of inhibition with respect to the intrinsic timescale of the individual neurons. More precisely, fast excitation favors synchrony whereas fast direct inhibition typically desynchronizes neurons [24].

* E-mail: ibelykh@gsu.edu
** E-mail: sjalil1@student.gsu.edu
*** E-mail: ashilnikov@gsu.edu

In-phase and anti-phase synchronized bursting are the key component for functioning of many neuronal networks, including Central Pattern Generators (CPGs) [36–39]. CPGs are small polymorphic neural circuits, governing various rhythmic activities including cardiac beating, cycles of basal ganglia, and animal locomotion [37–41]. CPG with a given neural circuitry can drive multiple behaviors and switch between different neuronal rhythms upon various conditions [42]. Examples include the Tritonia swim CPG [43], and switching between trot and gallop in several animals, respiratory movements, switching between crawling and swimming in leeches [40]. Switching between locomotion behaviors can be attributed to switching between various attractors of a CPG network. Each attractor is associated with a definite rhythm on a specific time scale. Such a multifunctional CPG contrasts to a dedicated CPG that is only capable of generating a single robust rhythm. Its multistability can be solely built upon the multistability of the individual neurons composing the network. Of special interest here is endogenous bursting, co-existing with tonic spiking in multistable interneurons [12]. The other cause of the polyrhythmical behaviors and co-existing motor outputs in the CPG is its network architecture [38–41, 46–49]. The network circuitry, the synaptic and intrinsic properties of neurons cooperate synergetically to produce various synchronous and anti-synchronous rhythms [16–35].

In 1911, studying animal locomotive behaviors, Graham Brown proposed the concept of the *half-center oscillator* as a pair of reciprocally connected neurons that inhibit each other and produce a cycle of alternating bursts of activity [44, 45]. The half-center oscillator is the fundamental building block of many CPGs. Depending on the intrinsic dynamics of component neurons, the half-center oscillator typically produces anti-phase bursting, when composed of endogenous busters, or interacting spiking neurons [50, 51]. The mechanisms that give rise to anti-phase bursting [16, 18] include the synaptic release mechanism, post-inhibitory rebound, and synaptic escape [18]. Reciprocal inhibition is known to produce half-center bursting, provided that inhibition is fast [16–19], i.e. the synaptic decay is faster than the duration of presynaptic drive. This carries over to larger interconnected inhibitory networks [18]. At the same time, a common fast inhibition of a neuronal network received from one or several pacemaker neurons was shown to favor synchronization [27]. It was also shown in [27] that a small amount of electrical coupling, added to already significant common inhibition of the network can increase the synchronization more than a very large increase in the synchronizing inhibitory coupling. Central pattern generators (CPGs) and other neural circuits are often composed of pairs of mutually inhibiting cells, driven by a common bursting pacemaker [43, 50]. Understanding the emergence of different anti-phase and synchronous rhythms in such networks requires an in-depth knowledge of the interplay among mutual internal inhibition, common external driving, and temporal characteristics of neurons composing the network.

In this paper, we review our results, regarding the onset of in-phase bursting in inhibitory networks [35, 49, 52], and demonstrate that weak common inhibition applied to a network of neurons with strong repulsive connections can induce in-phase synchronized bursting. We use the geometric dynamical systems methods to show that the weak synchronizing inhibition from the same pacemaker neuron can win out over much stronger desynchronizing connections within the network, provided that the pacemaker's duty cycle, the fraction of the period during which the neuron bursts, is sufficiently long. We discuss the bifurcations of a saddle-node periodic orbit, letting the pacemaker neuron have a longer duty cycle and therefore allowing the weak common inhibition to win the "David vs. Goliath" fight. We also prove that anti-phase bursting in the half-center oscillator with fast non-delayed inhibitory connections co-exists with stable in-phase synchronization that appears from a fairly wide set of initial conditions. We describe the emergent mechanism of in-phase synchronization and discuss the implications of the analysis for various types of bursting neurons.

2. THE MODEL

We start with a network of bursting neurons with fast inhibitory connections and choose a Hodgkin–Huxley type model of a leech heart interneuron [13] as an individual cell unit of the

network. The equations corresponding to this network are

$$\begin{aligned} C\dot{V}_i &= F(V_i, h_i, m_i) - (V_i - E_{\rm s}) \sum_{j=1}^{n} g_{ij}^{\rm s} \Gamma(V_j - \Theta_{\rm syn}), \\ \dot{h}_i &= G(V_i, h_i) = [f(500, 0.0325, V_i) - h_i]/\tau_{\rm Na}, \\ \dot{m}_i &= R(V_i, m_i) = [f(-83, 0.018 + V_{K2}^{\rm shift}, V_i) - m_i]/\tau_{\rm K2}, \quad i, j = \overline{1, n}, \end{aligned} \tag{2.1}$$

where $f(a, b, V_i) = 1/(1 + e^{a(V_i+b)})$ and

$$\begin{aligned} F(V_i, h_i, m_i) = -[30m_i^2(V_i + 0.07) + 8(V_i + 0.046) \\ +160h_i(V_i - 0.045)\{f(-150, 0.0305, V_i)\}^3 + 0.006]. \end{aligned}$$

Here, the ith neuron variables V_i, h_i, and m_i are the membrane potential, opening probabilities of the sodium and potassium channels, respectively. Due to the disparity of the time constants $\tau_{\rm Na} = 0.0405$ and $\tau_{\rm K2} = 0.9$, the system (2.1) possesses two characteristic time scales: the voltage and the sodium current are the fast variables, while the potassium current is a slow one. It is known that the dynamics of the individual slow-fast system composing the network is centered around stable manifolds formed by the limit sets of the fast subsystem. The model possesses two such manifolds constituting a skeleton of bursting activity: 2D spiking and 1D quiescent, $\rm M_{eq}$, manifolds, composed of limit cycles and equilibria of the fast system. The individual model exhibits square-wave bursting; the bursting solution traverses along and repeatedly jumps between these manifolds (see Fig. 1). In Fig. 1, the solid blue S-shape curve $\rm M_{eq}$ and the dark yellow surface $m' = 0$ are two nullclines of the fast and slow systems, respectively. They are often called fast and slow nullclines. By construction, a point of intersection of $\rm M_{eq}$ with the slow nullcline, $m' = 0$, is an equilibrium state of the corresponding neuron. Further details on the dynamics of uncoupled equations (2.1) can be found in [13]. Here, $V_{K2}^{\rm shift}$ is the intrinsic, bifurcation parameter governing the temporal characteristics of bursting cells.

In network (2.1), the synapses are fast and non-delayed [31]. The inhibitory synapses are described using *fast threshold modulation* (FTM), the kind of coupling that was proposed by Somers and Kopell [21, 53]. The synaptic coupling function is given by the sigmoidal function $\Gamma(V_j - \Theta_{\rm syn}) = 1/[1 + \exp\{\lambda(V_j - \Theta_{\rm syn})\}]$, where $\lambda = -1000$. The synaptic threshold $\Theta_{\rm syn} = -0.03$ is set so that every spike in the single neuron burst can cross the threshold (see Fig. 1). The synaptic current towards the post-synaptic cell is initiated when the pre-synaptic cell is above this threshold. The reversal potential $E_{\rm s} = -0.0625$ is set below the minimum values of V_i to ensure that the synapse is inhibitory.

3. HALF-CENTER OSCILLATOR: ANTI-PHASE BURSTING

Consider first a pair of bursting neurons (2.1) with reciprocally inhibitory couplings. This half-center network is known to solely produce anti-phase oscillations [18]. By geometry of the nullclines, each uncoupled cell has a single, unstable equilibrium state located away from the stable, hyperpolarized branch of $\rm M_{eq}$. The effect of inhibition from one cell to the other is to shift the S-shape nullcline $\rm M_{eq}$ towards the slow nullcline $m' = 0$ in the phase space of the inhibited cell. If inhibition is sufficient, this creates a new stable equilibrium around the lower knee of $\rm M_{eq}$ through a saddle-node bifurcation (Fig. 1). We will refer to this stable equilibrium state as a lock-down state. Cutting inhibition off makes this equilibrium state disappear through the reverse saddle-node bifurcation. This bifurcation has a remarkable feature of the bifurcation memory, revealed through a specific, scalable delay of the flight time of the phase point passing throughout a vicinity of the disappeared saddle-node. While spiking, the active cell keeps oscillating around the synaptic threshold $\Theta_{\rm syn}$, rapidly switching inhibition of the inactive cell on and off. Therefore, the inhibiting current emerges periodically for a period shorter than the characteristic escape time of the inactive cell. Hence, the latter is trapped and oscillates around the lower knee of the inhibited nullcline, depicted by the dotted blue line in Fig. 1. The active cell eventually reaches the end of the spiking

manifold and falls down to M_{eq}. This changes the governing nullcline for the other cell and releases it from inhibition. Therefore, the released cell jumps up and turns inhibition of the other cell on. This process of switching between active and inactive states of the two cells is cyclic and results in the onset of anti-phase bursting. A similar hold-then-release mechanism of the anti-phase behavior of spiking cells is often referred to as "synaptic release" [16, 18], causing post-inhibitory rebound [18].

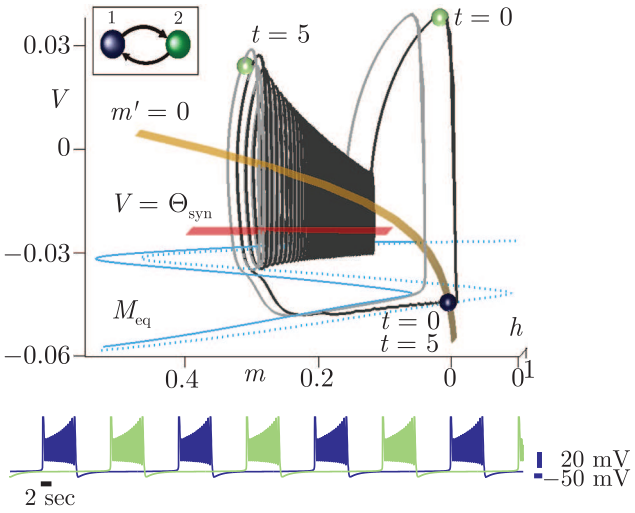

Fig. 1. Half-center oscillator composed of inhibitory neurons (2.1). $V_{K2}^{\text{shift}} = -0.02$. The inhibitory connections are strong ($g_{12}^{s} = g_{21}^{s} = 2$). (Top) The uncoupled and inhibited nullclines are depicted by solid and dotted blue lines, respectively. Color-matching balls represent the instant phase points of the cells on the bursting orbit. The dark gray trajectory corresponds to the anti-phase solution, while the light one is the reference trajectory of the uncoupled cell. As soon as the active (green) cell is above the threshold Θ_{syn}, the nulcline M_{eq} is shifted towards the slow nullcline $m' = 0$ to generate a stable equilibrium state near the lower knee through the saddle-node bifurcation. The inactive (blue) cell is trapped at it until the active cell falls down to M_{eq}. (Bottom) Time-series of the established anti-phase dynamics.

Below we show that the synaptic release mechanism along with a long duty cycle of driving neurons play the crucial role in inducing synchronization in larger networks.

4. THREE-CELL NETWORK: DAVID VS. GOLIATH

Inspired by the connectivity diagrams of a heart leech CPG [50] and a tritonia CPG governing locomotion [43], where neurons are organized in pairs of cells with strong reciprocal inhibition and each pair receives common inhibition from external neurons, we consider a three-neuron network shown in Fig. 2 (left inserts). In this network, code-named "David vs. Goliath," neurons 1 and 2 form a half-center oscillator, receiving common inhibition from neuron 3. The reciprocal inhibition within the pair is strong ($g_{12}^{s} = g_{21}^{s} \equiv g_{G}^{s}$), and the pair bursts in anti-phase in the absence of inhibition from neuron 3. Neuron 3 is assumed to have much (a hundred times) weaker unidirectional connections with the pair: $g_{31}^{s} = g_{32}^{s} \equiv g_{D}^{s}$ and $g_{13}^{s} = 0$, $g_{23}^{s} = 0$. In what follows, neuron 3 shall attempt to induce in-phase synchronized bursting in the half-center pair, fighting against a much stronger desynchronizing force within the half-center network. It is worth noticing that the "David vs. Goliath" ratio of the couplings is particularly pronounced in the tritonia CPG [43]. Let us consider two distinct outcomes of this "David vs. Goliath" fight, depending on the duty cycle of the driving neuron 3.

4.1. Case 1: Short Duty Cycle (< 50%)

Weak common inhibition is unable to establish synchronization within the "Goliath" network under this condition, and "David" always fails. The mechanism leading to the anti-phase bursting is similar to the above mechanism in the half-center oscillator.

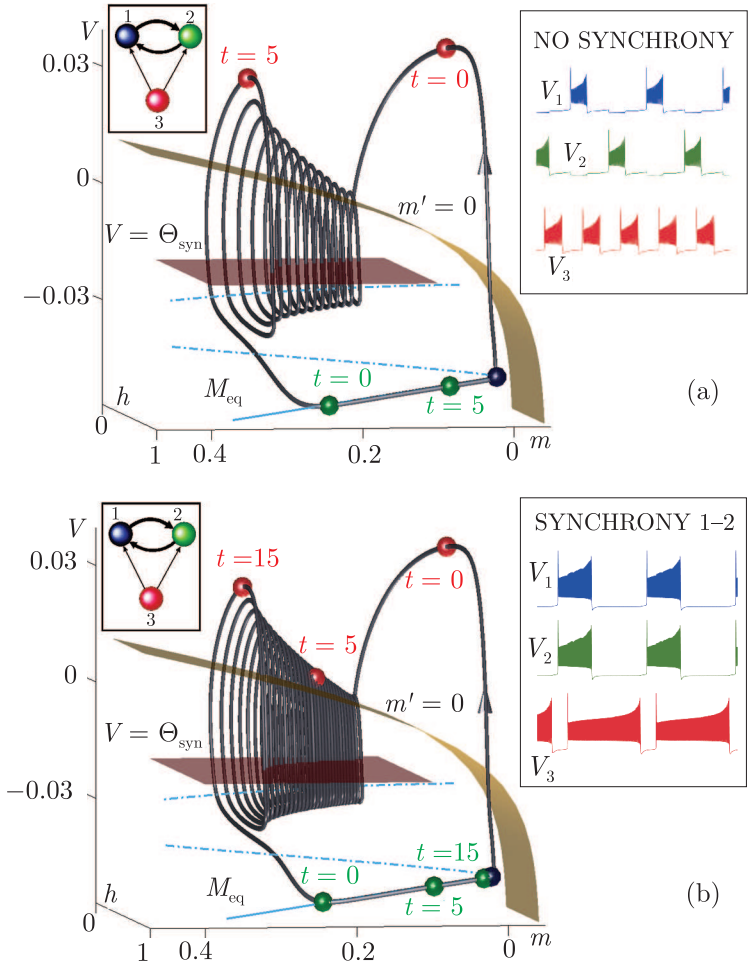

Fig. 2. Dynamics of the "David vs. Goliath" network (left insert) with weak $g_D = 0.02$ and strong coupling $g_G = 2$ for two distinct duty cycles. (a) Duty cycle at $V_{K2}^{shift} = -0.02$ is insufficient to lock neurons 1 and 2 down long enough to achieve burst synchronization. (b) Long burst duration at $V_{K2}^{shift} = -0.024$ allows the driven neurons to get together at the lock-down state near the saddle-node and to fire synchronously. This allows "David" to beat "Goliath".

Recall that due to the antiphase behavior, either cell of the "Goliath" network is always inactive, being locked down near the right knee of M_{eq}. While the phase state of the driving neuron 3 is on the spiking manifold M_{lc} above the threshold, it inhibits "Goliath" extending the lock-down state of the cell further. Note that in the 3D phase space of each individual system, the gap between the quiescent manifold M_{eq} and the slow nullcline $m' = 0$ is initially small so that a weak inhibition originating from the driving neuron is sufficient to close the gap and hence to lock either "Goliath" neuron down. Loosely speaking, this gap may be viewed as a narrow mountain gorge, where only 300 Spartans can hold off a vastly superior army. Figure 2a shows that at the given V_{K2}^{shift} the duty cycle of the driving neuron is not long enough to put both neurons 1 and 2 into the lock-down state. Neuron 1 (blue ball) is initially locked at the right knee by the driving neuron 3. At the same time, the phase point of neuron 2 (green ball) moves along M_{eq} towards its right knee, in attempt to catch up with the phase state of neuron 1. As soon as the phase point (red ball) of the driving neuron 3 eventually reaches the end of the spiking manifold and falls down to M_{eq}, this turns off the driving inhibition. Released from inhibition, neuron 1 is free to fire a spike, while neuron 2 remains yet inactive. After jumping up, the phase point of neuron 1 traverses the synaptic threshold to turn on the strong inhibition that leaves now neuron 2 locked down until neuron 1 is out of its active phase. This process of switching between active and inactive states of neurons 1 and 2 becomes cyclic and leads to asynchronous behavior of the "Goliath" network that they compose. Thus, an effort of the driving neuron 3 to break down the anti-phase firing rhythm of the

"Goliath" network fails. Moreover, the driving neuron 3 with a duty cycle shorter than about 45% cannot synchronize the given half-center pair, even if the strength of common inhibition exceeds that of reciprocal inhibition within the half-center network (see Fig. 3).

4.2. Case 2: Longer Duty Cycle

We set the driving neuron relatively close to the transition from bursting into tonic spiking which is due to either the blue sky bifurcation [13, 54, 55] or the Lukyanov–Shilnikov bifurcation of a saddle-node limit cycle with homoclinic orbits [12, 56]. In either case, the duty cycle grows fast as V_{K2}^{shift} approaches the transition value [13]. It is worth noticing that near the transition the burst duration becomes sensitive to small variations of the parameter and external contributions induced by synaptic currents. Close to a saddle-node bifurcation of a limit cycle on the spiking manifold, the system slows down and slowly passes the ghost preceding the emergence of the saddle-node limit cycle. This allows the driving neuron 3 to maintain long burst durations without changing the interburst interval. In other words, it spends more time on the spiking manifold than on the lower branch of the nullcline M_{eq}.

We start with the duty cycle of 80% which lies in a biologically plausible interval [50]. Fig. 2b illustrates the onset of in-phase synchronization between neurons 1 and 2, induced by the weak common inhibition. In contrast to the previous case of Fig. 2a, neuron 3 remains active much longer, letting the driven neurons get together and locking them at the right knee. When the two last cells are released from inhibition, they jump up together, giving rise to the in-phase synchronized rhythm. Their further behavior on the spiking manifold depends on the coupling parameters and synaptic threshold. For the above mentioned parameters, they remain completely synchronized. This is in contrast with the expectations that their phase trajectories would diverge as the strong desynchronizing connections between the two neurons are turned on. This surprising observation will be discussed in detail in the next Section.

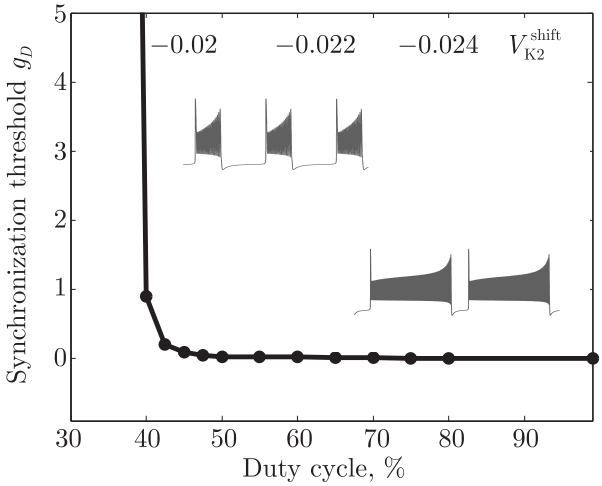

Fig. 3. Dependence of the threshold coupling strength g_{D}, inducing synchronization in the half-center network, on the duty cycle of the driving neuron 3. Other parameters are the same as in Fig. 2. Values of V_{K2}^{shift} correspond to the indicated duty cycles.

Fig. 3 shows a wide horizontal plateau in the duty cycle-dependence curve of the synchronization threshold coupling for duty cycles greater than 50%. This confirms that the strength of common inhibition plays no essential role in inducing synchronization, provided that it is sufficient to close the gap between the nullclines. The induced burst synchronization persists even when the driven neurons are mismatched due to both intrinsic properties of the cells and asymmetries of the network [49]. In particular, it persists even under a 200% mismatch between coupling strengths, like $g_{12} = 1$ and $g_{21} = 3$. Moreover, the inhibitory connections from neuron 3 do not have to be unidirectional; for example, symmetric synaptic couplings $g_{13} = g_{31} = 0.02$ and $g_{23} = g_{32} = 0.02$ also induce burst synchronization in the half-center network.

5. SYNCHRONIZED BURSTING: THE EVIL TWIN OF THE HALF-CENTER OSCILLATOR

The above burst-duration mechanism of in-phase synchronized bursting, induced by common inhibition, explains the onset of burst synchronization when neurons 1 and 2 start firing at the same time, after having released from common inhibition by neuron 3. However, the onset of complete synchronization when the states of the two neurons converge to each other on the spiking manifold remains a puzzle. In fact, the strong reciprocal inhibition connections between the two neurons are turned on while the common inhibition is turned off (neuron's 3 state still is on the lower branch of the nullcline). It shows that the half-center oscillator, composed by neurons 1 and 2, is capable of synchronizing by itself, provided that the neurons' states are brought close enough to each other and are on the spiking manifold. This is in contrast with the conventional belief as reciprocal inhibition is postulated to produce only anti-phase bursting, provided that inhibition is fast [16, 17, 20, 24], i.e. the synaptic decay is faster than or comparable to the duration of presynaptic drive.

In what follows, we will solve this puzzle and show that reciprocal inhibition can make completely synchronized bursting stable and robust [52]. This makes the half-center oscillator network bistable so that anti-phase bursting and the synchronous (in-phase) rhythm co-exist. In many cases, alternating anti-phase bursting is crucial in the occurrence of heart beats, and motor and locomotion rhythms. At the same time, synchronized firing is often considered to be an important part of the dysfunction of a biological system or a CPG. This is the reason for calling co-existent synchronized bursting the Evil Twin.

We consider the half-center oscillator network, modelled by the system (2.1) with $n = 2$ and $g^{\rm s}_{12} = g^{\rm s}_{21} \equiv g_{\rm s}$. Hence, the system (2.1) transforms into

$$\begin{aligned} &C\,\tfrac{dV_i}{dt} = F(V_i, h_i, m_i) - g_{\rm s}(V_i - E_{\rm s})\Gamma(V_j - \Theta_{\rm syn}),\\ &\tau_h \tfrac{dh_i}{dt} = G(V_i, h_i), \quad \tau_m \tfrac{dm_i}{dt} = R(V_i, m_i),\ i, j = 1, 2. \end{aligned} \tag{5.1}$$

We reveal the robustness of synchronized bursting with respect to transversal perturbations against phase mismatch between the two neurons. More specifically, we study how the basin of attraction of the synchronous solution depends on the phase along the synchronous orbit. The synchronous orbit is parameterized with respect to the phase from 0 to 360 degrees. The zero phase corresponds to the beginning of the quiescent period (see Figs. 4a and 4c). The width of the shaded region (the synchronization "river") in Fig. 4c gives the maximum size of the phase difference that provides stable synchronization at a given phase. Figure 4c shows that the beginning of the spiking phase of bursting corresponds to the widest synchronization zone. The synchronization zone narrows down towards the quiescent phase so that if the phase difference exceeds a critical value, anti-phase synchronization arises via the hold-and release mechanism, described in Section 3. Figure 4 demonstrates that stable synchronization is a typical phenomenon for half-center networks that appears from a wide set of initial conditions.

In the rest of the article, we explain the synchronizing effect of fast non-delayed reciprocal inhibition [52]. This is done by means of the variational equations for the transverse perturbations to the completely synchronous solution [31]:

$$\begin{aligned} C\dot{\xi} &= F_V(V,h,m)\xi + F_h(V,h,m)\eta + F_m(V,h,m)\zeta\\ &\quad +(S_1 + S_2)\xi\\ \tau_{\rm h}\dot{\eta} &= [G_V(V,h)\xi - \eta]\\ \tau_{\rm m}\dot{\zeta} &= [R_V(V,m)\xi - \zeta], \qquad \text{where} \end{aligned} \tag{5.2}$$

$$\begin{aligned} S_1 &= -g_s\Gamma(V - \Theta_{\rm syn})\\ S_2 &= g_s(V - E_{\rm s})\Gamma_V(V - \Theta_{\rm syn}) \end{aligned} \tag{5.3}$$

and $\xi = V_1 - V_2,\ \eta = h_1 - h_2,\ \zeta = m_1 - m_2$ are infinitesimal differences. The derivatives are calculated at the point $\xi = 0,\ \eta = 0,\ \zeta = 0$, and $\{V(t),\ h(t),\ m(t)\}$ corresponds to the synchronous

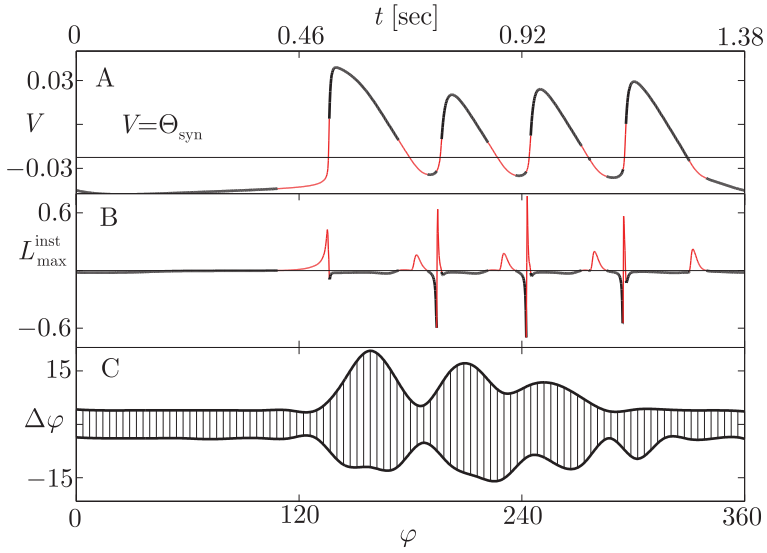

Fig. 4. (a) Voltage trace of synchronous bursting with four spikes. The synaptic threshold $V = \theta_{syn}$ is depicted by the line crossing the voltage trace. Thin and thick parts (red and black, online) of the voltage trace correspond to positive and negative values of the maximum instantaneous Lyapunov exponent, $L^{\rm inst}_{\rm max}$, respectively. Time scale of the burst period is shown on the top horizontal axis. All figures are aligned by phase, ϕ, which is shown on the lowest horizontal axis. Parameters of the network are $g_s = 0.4$, $\Theta_{syn} = -0.0225$, and $V^{\rm shift}_{K2} = -0.022$. (b) Magnitude of $L^{\rm inst}_{\rm max}$ oscillates between negative and positive values, that are, similar to (a), depicted by the thin and thick lines, respectively. The overall contribution $L^{\rm inst}_{\rm max}$, averaged over the period of the synchronous trajectory, is negative and synchronization is locally stable. (c) The dependence of the basin of attraction of synchronization on the phase along the bursting periodic orbit. The zero phase corresponds to the beginning of the quescient phase of bursting. The width of the shaded region (the synchronization "river") gives the maximum size of the phase difference that provides stable synchronization at a given phase.

bursting rhythm between the neurons defined via the self-connected system. The linearized system (5.2) has the coefficients that are time-dependent via the variable $V(t)$, $h(t)$, and $m(t)$, and the stability of the zero equilibrium of system (5.2) corresponds to the stability of the synchronous solution.

The two terms S_1 and S_2 are due to the inhibitory synaptic coupling. Note that the first term S_1 is always non-positive and therefore aims at *stabilizing* the zero equilibrium of system (5.2). Indeed, the sigmoidal function $\Gamma(V - \Theta_{\rm syn})$ is non-negative and ranges from 0 to 1, therefore adding $S_1\xi$ to the ξ-equation of system (5.2) has a stabilizing effect on the origin. More precisely, when the membrane potential $V(t)$ exceeds the threshold $\Theta_{\rm syn}$, the negative term S_1 is turned on and contributes to the stability of synchronization, as it were the case of excitatory coupling [31]. At the same time, the second coupling term S_2 is non-negative since $(V - E_{\rm s})$ is always positive (the synapses are inhibitory) and the graph of the derivative $\Gamma_V(V - \Theta_{\rm syn})$ has a bell shape with its high positive peak at $V = \Theta_{\rm syn}$ and rapidly declining tails. Consequently, the term $S_2\xi$, which is linear in ξ and has a positive cofactor S_2, tends to destabilize the zero equilibrium when the membrane potential $V(t)$ crosses or is close to the synaptic threshold $\Theta_{\rm syn}$. In other words, the inhibitory coupling plays a *dual* role in stabilizing and destabilizing synchronization as the terms S_1 and S_2 are competing between each other in attempt to make the synchronous solution stable or unstable, respectively. The impact of the inhibitory coupling on the stability of synchronization strongly depends on the location of the phase point on the synchronous bursting orbit.

When the membrane potential $V(t)$ is above the threshold $\Theta_{\rm syn}$, the synchronizing term S_1 is turned on and approaches to $-g_s$, whereas the desynchronizing, competing term S_2 rapidly decreases to zero while $V(t)$ increases and leaves a small transient region close to $V = \Theta_{\rm syn}$, where the contribution of S_2 is still significant. Thus, the overall contribution of the two terms, $S_1 + S_2$ for $V(t)$, exceeding the threshold $\Theta_{\rm syn}$ and the values from its small vicinity, is negative. Hence, similar to fast excitation, the inhibition tends to synchronize the cells along the bursting part of

the synchronous trajectory, above the values from the small vicinity of $\Theta_{\rm syn}$. On the other hand, when $V(t)$ crosses the threshold $\Theta_{\rm s}$, the desynchronizing term S_2 reaches its peak value which is significantly higher that the corresponding value of S_1. Thus, the desynchronizing term S_2 becomes decisive in the vicinity of $V = \Theta_{\rm s}$. The width of this vicinity region is defined by the parameter $\lambda = -1000$, showing how close the sigmoidal function $\Gamma(V - \Theta_{\rm syn})$ is to the Heaviside function. In the case of the Heaviside function, the size of this vicinity region shrinks to zero.

In other words, every time the synchronous trajectory crosses the vicinity of $V = \Theta_{\rm syn}$, it receives a strong, but short-term desynchronizing impact due to S_2, causing an increase in the transversal perturbations. However, during the fraction of time the system is above the threshold and its small vicinity, the inhibition plays a synchronizing role and the synchronous orbit receives a weaker, but longer lasting synchronizing impact due to S_1, so that the perturbations temporarily decrease. This is depicted in Figs. 4a and 4b, reporting the numerical calculations of the instantaneous values of the least stable transversal Lyapunov exponent, $L^{\rm inst}_{\rm max}$ of the synchronous trajectory, calculated via the stability system (5.2). It is shown in Fig. 4a that the location of the points on the bursting part of the synchronous trajectory, that correspond to a negative instantaneous Lyapunov exponent coincides with the region above the threshold vicinity region, where the overall contribution of S_1 and S_2 is negative. This part of the trajectory with a negative instantaneous Lyapunov exponent is depicted by the thick line. The thin line corresponds to the part of the trajectory with a positive instantaneous Lyapunov exponent that lies in the threshold vicinity region where the desynchronizing term S_2 dominates over S_1. Note that the quiescent part of the synchronous orbit, corresponding to the wide horizontal plateau in Fig. 4a, contains regions with negative and positive instantaneous Lyapunov exponents that oscillate around and are very close to 0. Here, the contribution of the coupling is almost negligible since the cells are significantly below the synaptic threshold $V = \Theta_{\rm syn}$ and the coupling is turned off so that the variations in the sign of the instantaneous Lyapunov exponent are caused by the time-varying Jacobian of the uncoupled system. Figure 4b shows the magnitude of the instantaneous Lyapunov exponent $L^{\rm inst}_{\rm max}$ that indicates its local contribution towards the overall stability of synchrony. The positive peaks in $L^{\rm inst}_{\rm max}$, correspond to the sharp appearance of the desynchronizing term S_2 when the synchronous orbit crosses the threshold.

The threshold value $\Theta_{\rm syn}$ and the synaptic strength $g_{\rm s}$ are two crucial factors that determine the stability of the variational equations (5.2), and, therefore, the stability of synchronization. The choice of $\Theta_{\rm syn}$ affects the balance between the competing terms S_1 and S_2 and may reverse the overall contribution of the coupling from negative to positive and vice versa. For instance, raising the threshold to the upper part of the bursting trajectory decreases the contribution of the term S_1 and leads to desynchronization (see Fig. 5). On the other hand, lowering the threshold makes the overall contribution of S_1 stronger as it remains switched on during a longer fraction of the burst. However, when the threshold $\Theta_{\rm syn}$ is lowered further so that it is tangent to the lowest part of the bursting trajectory, the desynchronizing term S_2 remains switched on longer due to the tangency (see Fig. 5c). Hence, the desynchronizing term S_2 wins over the synchronizing term S_2 and synchrony becomes unstable (see Figs. 5a and 5b).

Figure 5a shows the dependence of the Lyapunov exponent $L_{\rm max}$ on the synaptic threshold $\Theta_{\rm syn}$ for a fixed synaptic strength g_s. It is shown that there are two intervals of Θ_{syn}, corresponding to negative Lyapunov exponents, and, therefore, to locally stable synchronization of bursting neurons (2.1).

It is worth noticing that the values of Θ_{syn} from the left interval of stability (see Fig. 5a) lie between -0.038 to -0.036. For these values, the threshold Θ_{syn} is placed below the minimum value of spikes and cannot intersect the bursting part of the trajectory and, hence, cannot account for interaction with the presynaptic neuron, while the latter is in the tonic spiking phase. As far as the synaptic coupling between the neurons is concerned, this location of the synaptic threshold Θ_{syn} implies an interaction that is similar to that between spiking (non-bursting) cells [18] such as Morris–Lecar or FitzHugh–Nagumo spiking neurons. Here, the synaptic coupling is always switched on when the neurons are on the tonic spiking manifold and switched off when the neurons are on the quiescent branch of the solution. This is another surprising implication of this work, showing that bursting cells with the FTM reciprocal inhibition can still achieve stable synchrony provided that they are only connected in a way similar to non-bursting cells. Here, the neurons feel the

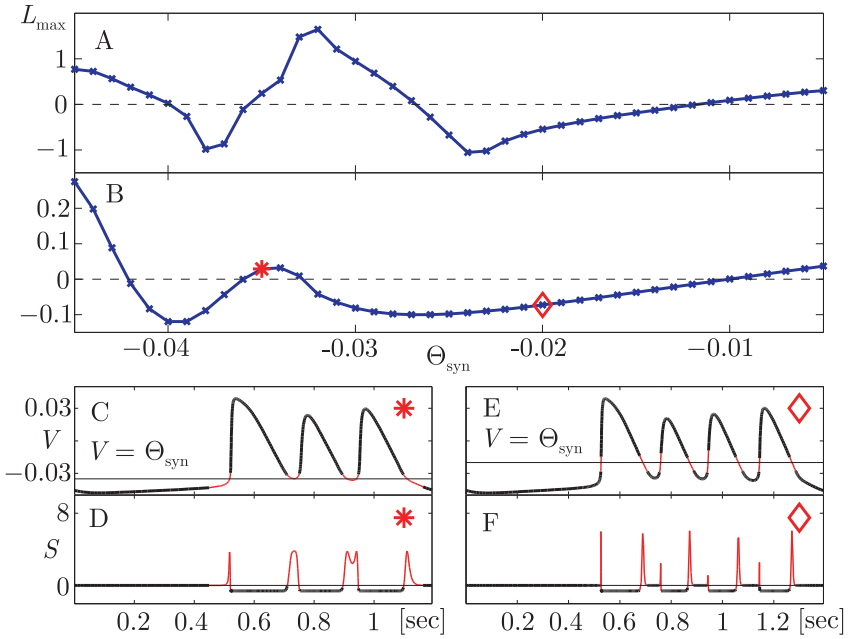

Fig. 5. Stability of synchronization as a function of the synaptic threshold Θ_{syn}. (a) Lyapunov exponent $L_{\max}$ is plotted versus Θ_{syn} for a fixed value $g_s = 0.3$. Note two intervals of stability indicated by negative Lyapunov exponents. The left interval of stability, ranging from $\Theta_{syn} = -0.038$ to $\Theta_{syn} = -0.036$, indicate lower thresholds Θ_{syn} where spikes do not cross the threshold Θ_{syn}. The right interval corresponds to the thresholds Θ_{syn}, intersecting the spikes. (b) Dependence of the averaged sum $\langle S\rangle = \langle S_1 + S_2\rangle$ on the threshold Θ_{syn}. The graph of $\langle S\rangle$ follows that for the Lyapunov exponent. In the physiologically relevant interval of Θ_{syn}, ranging from -0.02 to 0.015, the curve for $\langle S\rangle$ agrees with the Lyapunov exponent curve remarkably well. (c,d and e,f) Plots similar to Figs. 4a and 4b for two values of the synaptic threshold $V = \Theta_{syn}$, corresponding to unstable (c,d) and stable (e,f) synchronization. The asterix and diamond indicate the two values chosen on the graph $L_{\max}$. (d) When the threshold Θ_{syn} is tangent to the lowest part of the spikes (c), the desynchronizing term $\langle S_2\rangle$ remains turned on for longer periods of time, so that $\langle S\rangle$ becomes positive, making in-phase synchronization unstable. (e) When Θ_{syn} crosses the spikes transversally, the impact of the desynchronizing term S_2 is weaker and $\langle S\rangle$ is negative enough to ensure stable synchronization.

interaction only during two fast transitions between quiescence and the spiking phase of bursting that are the only time instants when the neurons' voltages can hit the synaptic threshold Θ_{syn} [18].

Figure 5b presents the dependence of the sum $\langle S\rangle = \langle S_1 + S_2\rangle$, averaged over the period of the synchronized bursting trajectory, on the threshold Θ_{syn}. The graph of $\langle S\rangle$ resembles the stability curve in Fig. 5a; there is no exact peak-to-peak coincidence between the two curves, especially within an interval of Θ_{syn} close to the minimum values of spikes. So for $\Theta_{syn} = -0.03$, the average $\langle S\rangle$ is negative, whereas the Lyapunov exponent $L_{\max}$ is still positive, and hence synchronization is unstable, despite the overall stabilizing effect of inhibition. This is due to a very strong instability of the uncoupled system near $V - 0.03$ which is the third crucial factor affecting the stability of synchronization. In a physiologically relevant interval of the thresholds Θ_{syn} between -0.02 and 0.01 (see [50, 51]), intersecting the burst in a middle of spikes, the curve for $\langle S\rangle$ in Fig. 5b agrees with the Lyapunov exponent curve in Fig. 5a remarkably well. In particular, it predicts the value $\Theta_{syn} = -0.009$ at which synchronization loses its stability.

6. CONCLUSIONS

We have shown that the duty cycle of neurons driving an inhibitory network is the critical characteristic, determining the cooperative properties of the network. In strongly heterogeneous networks of non-identical neurons, the ratio of the duty cycles becomes the imperative order parameter that controls the dynamics of the network and designates its pacemaker by the intrinsic properties, or by the network structure. The pacemaker, being the longest bursting cell, makes other strongly uncorrelated neurons synchronized and determines the network's paces and rhythms.

Moreover, excitatory coupling added to the inhibitory network can essentially increase the burst duration of the given neuron. This allows the neuron to become a pacemaker and induce synchronous rhythms in the network by the above described mechanism. The role of excitatory coupling was discussed in [49]. The effect of the emergent network behavior shows how single neurons initially having shorter duty cycles can *self-organize* to create a pacemaker with a longer duty cycle that, in turn, induces network's synchronous rhythms. Uneven common inhibition of a neuronal network was also shown [49] to cause multiple, co-existent synchronous patterns, called polyrhythms, to emerge among the networked neurons. The discovered mechanism of induced synchronization is generic and applicable to other Hodgkin–Huxley–type neurons, capable of forming a half-center oscillator. It demonstrates how neurons with different duty cycles can be employed as building elements for constructing complex neuronal networks with prescribed cooperative behaviors.

We have discovered that anti-phase bursting in the half-center oscillator with fast non-delayed inhibitory connections, which had been believed to be the only robust rhythm, is accompanied by stable in-phase synchronization that appears from a fairly wide set of initial conditions. Should one neuron be initially in the bursting phase, whereas the other is in quiescence, fast non-delayed reciprocal inhibition between the cells leads to anti-phase bursting. However, if the neurons start firing in the tonic spiking phase, then the inhibition, instead of diverging them, will force the neurons' states to come together, resulting in stable synchronized bursting. Surprisingly, the onset of anti-phase bursting from initial conditions, corresponding to the tonic spiking phase of both neurons is improbable. Once anti-phase bursting is achieved, it remains resistant to external voltage perturbations of either neuron. On the contrary, even a weak common inhibition of both neurons can break the anti-phase regime and make the neurons burst together [35]. The role of the common inhibition in making in-phase synchronization stable is to bring the neurons' states relatively close to each other so that the reciprocal inhibition between the neurons could synchronize them.

We believe that our study of the synchronization mechanism of reciprocal inhibition and co-existing dynamical rhythms may help one better understand multi-stability and switching mechanisms between various neuronal rhythms of a multi-functional CPG upon various dynamical conditions and inputs.

ACKNOWLEDGMENTS

This work was supported by the GSU Brains and Behavior program (grant: "Dynamical principles of multifunctional central pattern generators") and the RFFI grants N 2100-065268 and N 09-01-00498-a.

REFERENCES

1. Rinzel, J., Bursting Oscillations in an Excitable Membrane Model, *Ordinary and Partial Differential Equations (Dundee, 1984)*, B. D. Sleeman and R. J. Jarvis (Eds.), Lecture Notes in Math., vol. 1151, New York: Springer, 1985, pp. 304–316.
2. Rinzel, J., A Formal Classification of Bursting Mechanisms in Excitable Systems, *Mathematical Topics in Population Biology, Morphogenesis and Neuroscience*, E. Teramoto and M. Yamaguti (Eds.), Lecture Notes in Biomath., vol. 71, Berlin: Springer, 1987, pp. 267–281.
3. Rinzel, J. and Ermentrout, B., Analysis of Neural Excitability and Oscillations, *Methods of Neural Modeling: From Synapses to Networks*, C. Koch and I. Segev (Eds.), MIT Press, 1989, pp. 135–169.
4. Ermentrout, G. B. and Kopell, N., Parabolic Bursting in an Excitable System Coupled with a Slow Oscillation, *SIAM J. Appl. Math.*, 1986, vol. 46, pp. 233–253.
5. Terman, D., Chaotic Spikes Arising from a Model of Bursting in Excitable Membranes, *SIAM J. Appl. Math.*, 1991, vol. 51, pp. 1418–1450.
6. Wang, X. J., Genesis of Bursting Oscillations in the Hindmarsh–Rose Model and Homoclinicity to a Chaotic Saddle, *Phys. D*, 1993, vol. 62, nos. 1–4, pp. 263–274.
7. Bertram, R., Butte, M. J., Kiemel, T., and Sherman, A., Topological and Phenomenologial Classication of Bursting Oscillations, *Bull. Math. Biol.*, 1995, vol. 57, pp. 413–439.
8. Izhikevich, E., Neural Excitability, Spiking and Bursting, *Internat. J. Bifur. Chaos Appl. Sci. Engrg.*, 2000, vol. 10, pp. 1171–1266.
9. Belykh, V. N., Belykh, I. V., Colding-Joregensen, M., and Mosekilde, E. Homoclinic Bifurcations Leading to Bursting Oscillations in Cell Models, *Eur. Phys. J. E. Soft Matter Biol. Phys.*, 2000, vol. 3, pp. 205–219.
10. Doiron, B., Laing, C., and Longtin, A., Ghostbursting: A Novel Neuronal Burst Mechanism, *Comput. Neurosci.*, 2002, vol. 12, pp. 5–25.

11. Shilnikov, A. and Cymbalyuk, G., Homoclinic Bifurcations of Periodic Orbits en route from Tonic-Spiking to Bursting in Neuron Models, *Regul. Chaotic Dyn.*, 2004, vol. 9, pp. 281–297.
12. Shilnikov, A., Calabrese, R., and Cymbalyuk, G., Mechanism of Bi-Stability: Tonic Spiking and Bursting in a Neuron Model, *Phys. Rev. E*, 2005, vol. 71, 056214, 9 p.
13. Shilnikov, A. and Cymbalyuk, G., Transition between Tonic-Spiking and Bursting in a Neuron Model via the Blue-Sky Catastrophe, *Phys. Rev. Lett.*, 2005, vol. 94, 048101, 4 p.
14. Fröhlich, F. and Bazhenov, M., Coexistence of Tonic Firing and Bursting in Cortical Neurons, *Phys. Rev. E*, 2006, vol. 74, 031922, 7 p.
15. Chanell, P., Cymbalyuk, G., and Shilnikov, A., Origin of Bursting through Homoclinic Spike Adding in a Neuron Model, *Phys. Rev. Lett.*, 2007, vol. 98, 134101, 4 p.
16. Wang, X.-J. and Rinzel, J., Alternating and Synchronous Rhythms in Reciprocally Inhibitory Model Neurons, *Neural Comput.*, 1992, vol. 4, pp. 84–97.
17. Van Vreeswijk, C., Abbott, L. F., and Bard Ermentrout, G., When Inhibition Not Excitation Synchronizes Neural Firing, *Comput. Neurosci.*, 1994, vol. 1, pp. 313–321.
18. Kopell, N. and Ermentrout, G. B., Mechanisms of Phase-Locking and Frequency Control, *Handbook of Dynamical Systems*, vol. 2, B. Fiedler (Ed.), Amsterdam: Elsevier, 2002, pp. 3–54.
19. Elson, R. C., Selverston, A. I., Abarbanel, H. D. I., and Rabinovich, M. I., Inhibitory Synchronization of Bursting Inbiological Neurons: Dependence on Synaptic Time Constant, *J. Neurophysiol.*, 2002, vol. 88, pp 1166–1176.
20. Golomb D. and Rinzel, J., Clustering in Globally Coupled Inhibitory Neurons, *Phys. Rev. E*, 1993, vol. 48, pp. 4810–4814.
21. Somers, D. and Kopell, N., Rapid Synchronization through Fast Threshold Modulation, *Biol. Cybernet.*, 1993, vol. 68, pp. 393–407.
22. Sherman, A., Anti-Phase, Asymmetric, and Aperiodic Oscillations in Excitable Cells: 1. Coupled Bursters, *Bull. Math. Biol.*, 1994, vol. 56, pp. 811–835.
23. Terman, D., Kopell, N., and Bose, A., Dynamics of Two Mutually Coupled Slow Inhibitory Neurons, *Phys. D*, 1998, vol. 117, pp. 241–275.
24. Rubin, J. and Terman, D., Synchronized Activity and Loss of Synchrony among Heterogeneous Conditional Oscillators, *SIAM J. Appl. Dyn. Sys.*, 2002, vol. 1, pp. 146–174.
25. Lewis, T. and Rinzel, J., Dynamics of Spiking Neurons Connected by Both Inhibitory and Electrical Coupling, *Comput. Neurosci.*, 2003, vol. 14, pp. 283–309.
26. Rubin, J. and Terman, D., Geometric Singular Perturbation Analysis of Neuronal Dynamics, *Handbook of Dynamical Systems*, vol. 2, B. Fiedler (Ed.), Amsterdam: Elsevier, 2002, pp. 93–146.
27. Kopell, N. and Ermentrout, G. B., Chemical and Electrical Synapses Perform Complementary Roles in the Synchronization of Interneuronal Networks, *Proc. Natl. Acad. Sci. USA*, 2004, vol. 101, pp. 15482–15487.
28. Bondarenko, V. E., Cymbalyuk, G. S., Patel, G., DeWeerth, S.P., and Calabrese, R. L., Bifurcation of Synchronous Oscillations into Torus in a System of Two Reciprocally Inhibitory Silicon Neurons: Experimental Observation and Modeling, *Chaos*, 2004, vol. 14, pp. 995–1003.
29. Bem, T. and Rinzel, J., Short Duty Cycle Distabilizes a Half-Center Oscillator, by Gap Junctions Can Restabilize the Anti-Phase Pattern, *J. Neurophysiol.*, 2004, vol. 91, pp. 693–703.
30. Cymbalyuk, G. S., Nikolaev, E. V., and Borisyuk, R. M., In-Phase and Anti-Phase Self-Oscillations in a Model of Two Electrically Coupled Pacemakers, *Biol. Cybernet.*, 1994, vol. 71, pp. 153-–160.
31. Belykh, I., de Lange, E., and Hasler, M., Synchronization of Bursting Neurons: What Matters in the Network Topology, *Phys. Rev. Lett.*, 2005, vol. 94, 188101, 4 p.
32. Izhikevich, E. M., Synchronization of Elliptic Bursters, *SIAM Rev.*, 2001, vol. 43, no. 2, pp. 315–344.
33. Van Vreeswijk, C. and Hansel, D., Patterns of Synchrony in Neural Networks with Spike Adaptation, *Neural Comput.*, 2001, vol. 13, pp. 959–992.
34. Rabinovich, M. I., Varona, P., Selverston, A. I., and Abarbanel, H. D. I., Dynamical Principles in Neuroscience, *Rev. Modern Phys.*, 2006, vol. 78, no. 4, pp. 1213–1265.
35. Belykh, I. and Shilnikov, A., When Weak Inhibition Synchronizes Strongly Desynchronizing Networks of Bursting Neurons, *Phys. Rev. Lett.*, 2008, vol. 101, 078102, 4 p.
36. Kopell, N., Toward a Theory of Modelling Central Pattern Generators, *Neural Control of Rhythmic Movements in Vertebrates*, A. H. Cohen, S. Rossignol, and S. Grillner (Eds.), New York: Wiley, 1987, pp. 369–413.
37. Getting, P. A., Emerging Principles Governing the Operation of Neural Networks, *Annu. Rev. Neurosci.*, 1989, vol. 12, pp. 185–204.
38. Marder, E. and Calabrese, R. L., Principles of Rhythmic Motor Pattern Generation, *Physiol. Rev.*, 1996, vol. 76, no. 3, pp. 687–717.
39. Marder, E., Kopell, N., and Sigvardt, K., How Computation Aids in Understanding Biological Networks, *Neurons, Networks, and Motor Behavior*, P. S. G. Stein, A. Selverston, S.Grillner, and D. G. Stuart (Eds.), Cambridge: MIT Press, 1998, pp. 139–150.

40. Kristan, W. B., Calabrese, R. L., and Friesen, W. O., Neuronal Control of Leech Behavior, *Progr. Neurobiol.*, 2005, vol. 76, pp. 279–327.
41. Kristan, W. B., and Katz, P., Form and Function in Systems Neuroscience, *Curr. Biol.*, 2006, vol. 16, R828–R831.
42. Briggman, K. L. and Kristan, W. B., Multifunctional Pattern-Generating Circuits, *Annu. Rev. Neurosci.*, 2008, vol. 31, pp. 271–294.
43. Katz, P. S., Tritonia, http://www.scholarpedia.org/article/Tritonia.
44. Brown, T. G., The Intrinsic Factors in the Act of Progerssion in the Mammal, *Proc. R. Soc. Lond. B*, 1911, vol. 84, pp. 308–319.
45. Brown, T.G., On the Nature of the Fundamental Activity of the Nervous Ventres: Together with an Analysis of the Conditioning of Rhythmic Activity in Progression, and a Theory of the Evolution of Function in the Nervous System, *J. Physiol.*, 1914, vol. 48, pp. 18-–46.
46. Canavier, C. C., Baxter, D. A., Clark, J. W., and Byrne, J. H., Control of Multistability in Ring Circuits of Oscillators, *Biol. Cybernet.*, 1999, vol. 80, pp. 87–102.
47. Baxter, D. A., Lechner, H. A., Canavier, C. C., Butera, R. J., Franceschi, A. A., Clark, J. W., and Byrne, J. H., Coexisting Stable Oscillatory States in Single Cell and Multicellular Neuronal Oscillators, *Oscillations in Neural Systems*, D. S. Levine, V. R. Brown, V. T. Shirey (Eds.), Hillsdale, NJ: Erlbaum Associates, 1999, pp. 51–78.
48. Prinz, A. A., Bucher, D., and Marder, E., Similar Network Activity from Disparate Circuit Parameters, *Nature Neurosci.*, 2004, vol. 7, pp. 1345–1352.
49. Shilnikov, A., Gordon, R., and Belykh, I., Polyrhythmic Synchronization in Bursting Network Motifs, *Chaos*, 2008, vol. 18, 037120, 13 p.
50. Cymbalyuk, G. S., Gaudry, Q., Masino, M. A., and Calabrese, R. L., Bursting in Leech Heart Interneurons: Cell Autonomous and Network Based Mechanisms, *J. Neurosci.*, 2002, vol. 22, pp. 10580–10592.
51. Tobin, A.-E. and Calabrese, R. L., Endogenous and Half-Center Bursting in Morphologically-Inspired Models of Leech Heart Interneurons, *J. Neurophysiol.*, 2006, vol. 96, pp. 2089–2106.
52. Jalil, S., Belykh, I., and Shilnikov, A., Fast Reciprocal Inhibition Can Synchronize Bursting Neurons, submitted for publication in *Phys. Rev. E.*
53. De Lange, E. and Kopell, N., Fast Threshold Modulation, Scholarpedia,
54. Turaev, D. V. and Shilnikov, L. P., Blue Sky Catastrophe, *Dokl. Math.*, 1995, vol. 51, pp. 404–407.
55. Shilnikov, A., Shilnikov, L. P., and Turaev, D.V., Blue Sky Catastrophe in Singularly Perturbed Systems, *Mosc. Math. J.*, 2005, vol. 5, no. 1, pp. 269–282.
56. Lukyanov, V. and Shilnikov, L. P., On Some Bifurcations of Dynamical Systems with Homoclinic Structures, *Dokl. Akad. Nauk SSSR*, 1978, vol. 243, no. 1, pp. 26–29 [*Soviet Math. Dokl.*, 1978, vol. 19, 1314–1318].